# Structure-property relationships of novel phosphonate-functionalized networks and gels of poly(β-amino esters)

Seckin Altuncu [a], Fatma Demir Duman [b], Umit Gulyuz [c, d], Havva Yagci Acar [b], Oguz Okay [d], Duygu Avci [a]

[a]Department of Chemistry, Bogazici University, Bebek 34342, Istanbul, Turkey
[b]Department of Chemistry, Koc University, Sariyer 34450, Istanbul, Turkey
[c]Department of Chemistry, Istanbul Technical University, Maslak 34469, Istanbul, Turkey
[d]Department of Chemistry and Chemical Processing Technologies, Kirklareli University, Luleburgaz 39750, Kirklareli, Turkey

Correspondence to: D. Avci (E-mail: avcid@boun.edu.tr)

Telephone: +90 212 359 4769.

## Abstract

pH sensitivity, biodegradability and high biocompatibility make poly(β-amino esters) (PBAEs) important biomaterials with many potential applications including drug and gene delivery and tissue engineering, where their degradation should be tuned to match tissue regeneration rates. Therefore, we synthesize novel phosphonate-functionalized PBAE macromers, and copolymerize them with polyethylene glycol diacrylate (PEGDA) to produce PBAE networks and gels. Degradation and mechanical properties of gels can be tuned by the chemical structure of phosphonate-functionalized macromer precursors. By changing the structure of the PBAE macromers, gels with tunable degradations of 5-97% in 2 days are obtained. Swelling of gels before/after degradation is studied, correlating with the PBAE identity. Uniaxial compression tests reveal that the extent of decrease of the gel cross-link density during degradation is much pronounced with increasing amount and hydrophilicity of the PBAE macromers. Degradation products of the gels have no significant cytotoxicity on NIH 3T3 mouse embryonic fibroblast cells.

**Keywords:** poly (β-amino esters); biodegradable polymer; phosphonate; mechanical properties

## 1. Introduction

Photopolymerizable biodegradable materials have been used in a wide range of biomedical applications such as tissue engineering and drug delivery because of their advantages of in vivo curing and no requirement of removal surgery [1-5]. Synthetic polymers have been utilized due to their adjustable chemical, physical and biological properties such as hydrophobicity, surface charge, degradation, porosity, mechanical properties and cell adhesion behavior [6-7].

Poly(β-amino ester)s (PBAEs) are an important class of biodegradable synthetic polymers which are being investigated as gene [8-15] and drug [16-21] delivery vehicles and tissue engineering scaffolds [22-34] due to their pH sensitivities, biodegradabilities and high biocompatibilities. They are easily prepared by Michael addition of difunctional amines to commercial diacrylates under mild conditions and are degradable to diols, bis(β-aminoacids), and poly(acrylic acid) chains under physiological conditions by cleavage of ester linkages due to hydrolysis. Acrylate terminated PBAEs can be easily prepared using acrylate/amine molar ratios > 1 and can be photopolymerized into degradable networks. To illustrate, a combinatorial approach was used to synthesize PBAE gels with a wide range of degradation times and mechanical properties for tissue engineering applications [22]. The effects of macromer structure and molecular weight on network properties such as degradation rate, mechanical properties and cell interactions were investigated [23,24]. The influence of macromer branching investigated by adding a trifunctional monomer showed a dose dependent improvement in network properties such as compressive modulus, tensile modulus and $T_g$ [25]. Some PBAE macromers were electrospun into scaffolds with diverse properties [26,27]. Fast degrading PBAE gels were used as porogens in a slower degrading PBAE matrix to generate scaffolds for

tissue growth [29]. Trigger-responsive PBAE hydrogels with acid sensitive and reduction responsive diacrylates were utilized for protein encapsulation [30].

Although properties such as the chemical structure of PBAE macromer, its molecular weight, branching etc. allow customization of network properties, the gels still undergo degradation and lose their mechanical properties too fast for most biomedical applications. One way to match the gels' properties to a desired application is to prepare their copolymers or composites. For example, PBAE macromers were used as crosslinkers for the synthesis of 2-hydroxyethyl methacrylate (HEMA) and N-vinylpyrrolidone (NVP) hydrogels to enhance the hydrogels' swelling and degradation properties [31]. Semi-degradable polymer networks, copolymers of PBAE macromers and methyl methacrylate, were prepared to control and enhance mechanical properties during degradation [32,33]. It was shown that as the low $T_g$ component degrades, the $T_g$ of the network and hence its modulus increases to give materials with tailorable toughness. Calcium sulfate/PBAE biodegradable hydrogel composites were developed to help vertical bone regeneration by preventing soft tissue infiltration [34].

Phosphorous-based materials have been widely used in the biomedical field due to their biodegradable, hemocompatible and protein resistant nature [35]. Incorporation of phosphorous containing groups to polymeric networks extends their application areas due to their strong interaction with hydroxyapatite-based tissue [36-39] and enhances their cell adhesion, [40-45] swelling and thermal properties. Recently, we have reported the effect of the phosphonate and bisphosphonate group on PBAE network properties [46-48]. Phosphonate-functionalized PBAE macromers were synthesized through reaction of various diacrylates and a primary phosphonate-functionalized amine (diethyl 2-aminoethylphosphonate). It was found that their gels, except polyethylene glycol diacrylate (PEGDA)-based ones, support the attachment of a larger number of SaOS-2 cells than nonphosphonated ones [46]. Bisphosphonate-functionalized PBAE gels with different chemistries exhibited similar degradation behavior, indicating that the hydrophilic nature of the bisphosphonate functional groups dominates all the

other effects and leads to the high mass loss. These macromers were used as crosslinkers for the synthesis of HEMA hydrogels, conferring small and customizable degradation rates upon them [47].

Although PEGDA hydrogels are one of the most widely studied biomaterials due to their biocompatibility and bioinertness, they have very slow degradation in vivo and hence are unsuitable for long-term implant applications. Therefore, it is desirable to adjust their degradation by functionalization to match tissue regeneration rates. In this study, we have synthesized novel phosphonate-functionalized PBAE macromers through Michael addition of a new difunctional phosphonated secondary amine and three different diacrylates with various hydrophilic/hydrophobic properties. The macromers were then copolymerized with PEGDA, to form gels with tunable degradation and mechanical properties. We focus on the effect of the chemical structure of PBAE macromers on gel properties such as swelling and degradation. Moreover, for the first time in the literature, we have also studied the mechanical properties of the gels as a function of the type and the amount of the macromers. As will be seen below, we were able to tune the degradation rate of gels and their cross-link density by changing the amount and hydrophilicity of PBAE macromers, to match those desired for tissue engineering applications.

## 2. Materials and Methods

### 2.1. Materials

4,9-dioxa-1,12-dodecanediamine, diethyl vinylphosphonate, 1,6-hexanediol diacrylate (HDDA), poly(ethylene glycol) diacrylate (PEGDA, $M_n$ = 575 Da), 1,6-hexanediol ethoxylate diacrylate (HDEDA), 1,8-diazabicyclo[5.4.0]undec-7-ene (DBU) and 2,2-dimethoxy-2-phenylacetophenone (DMPA) were commercially available from Aldrich Chemical Co. and were used as received. Roswell Park Memorial Institute (RPMI) 1640 medium (with L-

glutamine and 25 mM HEPES), penicillin/streptomycin (pen-strep) and trypsin-EDTA were purchased from Multicell, Wisent Inc. (Canada). Fetal bovine serum (FBS) was obtained from Capricorn Scientific GmbH (Germany). Thiazolyl blue tetrazolium bromide (MTT) and phosphate buffered saline (PBS) tablets were provided by Biomatik Corp. (Canada). The 96-well plates were purchased from Nest Biotechnology Co. Ltd. (China). NIH 3T3 mouse embryonic fibroblast cells were a kind gift of Dr. Halil Kavakli (Department of Molecular Biology and Genetics, Koc University, Istanbul, Turkey).

### 2.2. Methods

$^{1}H$, $^{13}C$ and $^{31}P$ NMR spectra were measured with a Varian Gemini 400 spectrometer using deuterated chloroform ($CDCl_3$) or methanol (MeOD) as solvent. Chemical shifts ($\delta$) were reported as ppm downfield from tetramethylsilane (TMS) as an internal standard. Coupling constants (*J*) were given in hertz (Hz). IR spectra were obtained on a Thermo Scientific Nicolet 6700 FTIR spectrometer in the range of 4000–650 $cm^{-1}$. Potentiometric titrations were carried out using a WTW Inolab 720 pH meter and WTW SenTix 41 epoxy pH electrode at room temperature. Glass transition temperatures ($T_g$) of the macromers and gels were determined by using a differential scanning calorimeter (DSC, TA Instruments, Q100). The samples were analyzed at a heating rate of 10 °C/min and in a temperature range of -90–200 °C. Degradation studies were done using a VWR Incubating Mini Shaker operating at 37 °C and 200 rpm.

### 2.3. Synthesis of tetraethyl (7,12-dioxa-3,16-diazaoctadecane-1,18-diyl)bis(phosphonate) (PA)

Method 1

4,9-dioxa-1,12-dodecanediamine (0.5 g, 0.52 mL, 2.45 mmol) and diethyl vinylphosphonate (0.84 g, 0.79 mL, 5.15 mmol) were mixed at room temperature for two days. The mixture was

washed with hexane to remove unreacted diethyl vinylphosphonate and the pure product was obtained as colorless liquid in 85% yield.

Method 2

4,9-dioxa-1,12-dodecanediamine (0.5 g, 0.52 mL, 2.45 mmol) and diethyl vinylphosphonate (0.80 g, 0.75 mL, 4.89 mmol) were mixed in water (1.5 mL) at 85 °C for 45 min. After removal of water, the mixture was washed with hexane to remove unreacted starting materials and the pure product was obtained as colorless liquid in 74% yield.

$^{1}$H-NMR (400 MHz, $CDCl_3$, δ): 1.31 (t, $^{3}J_{HH}$ = 8 Hz, 12H, $CH_3$), 1.60 (m, 4H, C$H_2$-$CH_2$-NH), 1.74 (quint, $^{3}J_{HH}$ = 8 Hz, 4H, $CH_2$), 1.94 (m, 4H, $CH_2$-P=O), 2.68 (t, $^{3}J_{HH}$ = 8 Hz, 4H, $CH_2$-NH) 2.88 (m, 4H, C$H_2$-$CH_2$-P=O), 3.40 (t, $^{3}J_{HH}$ = 8 Hz, 4H, $CH_2$-O), 3.45 (t, $^{3}J_{HH}$ = 4 Hz, 4H, $CH_2$-O), 4.09 (m, 8H, $CH_2$-O-P=O) ppm. $^{13}$C-NMR (100 MHz, $CDCl_3$, δ): 16.35, 16.41 (d, $CH_3$), 25.68, 27.07 (d, $CH_2$-P=O), 26.30 ($CH_2$), 29.93 (*C*$H_2$-$CH_2$-NH), 43.23, 43.25 (d, NH-C$H_2$-$CH_2$-P=O), 46.86 ($CH_2$-NH), 61.51, 61.58 (d, $CH_2$-O-P=O), 69.09 ($CH_2$-O), 70.63 ($CH_2$-O) ppm. $^{31}$P-NMR (162 MHz, $CDCl_3$, δ): 30.47 ppm. FTIR (ATR): 3503 (N-H), 2935 (C-H), 1236 (P=O), 1022, 954 (P-O) $cm^{-1}$.

**2.4. Synthesis of PBAE macromers**

Method 1

The diacrylates (PEGDA, HDEDA or HDDA) and PA were mixed at a molar ratio of 1.1:1, 1.2:1 and 1.3:1 in 10 mL vials at room temperature for 4 days while stirring. If the stirring was stopped due to an increase in viscosity, a very small amount of dichloromethane (DCM) was added to the mixture and removed under reduced pressure after the reactions. The macromers were obtained as colorless viscous liquids in 78-85% yield after washing with petroleum ether (HDEDA and HDDA-based ones) or diethyl ether (PEGDA-based ones) to remove unreacted diacrylates, PA or monoaddition products; and dried under reduced pressure.

Method 2

PA (0.5 g, 0.94 mmol) and DBU (0.14 g, 0.14 mL, 0.94 mmol) were mixed in MeOH (1 mL). Then PEGDA (0.65 g, 0.58 mL, 1.13 mmol) was added and the mixture was stirred at room temperature for 12 h. After removal of MeOH, the residue was washed with diethyl ether to remove unreacted diacrylates, PA or monoaddition products; and dried under reduced pressure to give the product in 32-35 %.

### 2.5. $pK_b$ measurements

The $pK_b$ values of the macromers were determined by titration method. 50 mg of macromer was dissolved in deionized water to give a final concentration of 1.0 mg/mL. The pH of the macromer solutions was set to pH 2.0 using 2 M HCl and titrated to pH 11 with 0.1 M NaOH solution. The pH of solutions was measured after each addition using a pH meter (WTW Inolab pH 720) at room temperature. The $pK_b$ value was determined from the inflection point of the titration curve which responds to the pH value where 50% of protonated amine groups are neutralized.

### 2.6. Synthesis of PBAE gels

A 10 % (w/v) DMPA solution in DCM was added to a macromer-PEGDA mixture (80:20 or 50:50 w% PEGDA:macromer) to give a final concentration of 1 w% DMPA. After the removal of the solvent in a vacuum oven, the mixture was placed into a vial and polymerized in a photoreactor containing 12 Philips TL 8W BLB lamps, exposing it to UV light (365 nm) for 30 min. For comparison, the macromers alone were also polymerized under the same conditions. The polymer samples thus formed were weighed and immersed in ethanol for approximately 12 h to remove unreacted components. After drying in a vacuum oven until constant weight, the samples were weighed again (final mass). The gel fraction $W_g$, that is, the fraction of insoluble polymer, was calculated from the initial and final mass of the gel specimens.

### 2.7. Swelling Studies

Swelling studies were conducted by immersing dry gel samples (45±15 mg) into PBS (pH 7.4) solution at 37 °C. The samples were removed from the solution at pre-determined time intervals, blotted on filter paper and the swollen weight was measured. The increase in the weight of the samples was recorded as a function of time until equilibrium was reached. The degree of swelling ($Q$) was calculated using the equation:

$$Q = \frac{Ws - Wd}{Wd} x\ 100 \quad (1)$$

where $W_s$ and $W_d$ refer to the weight of swollen and dry samples respectively. The average data obtained from triplicate measurements were reported. The standard deviations were less than 5.2%.

### 2.8. Degradation studies

In vitro degradation of the gel samples as prepared above (45±15 mg, initial mass) were carried out in PBS (pH 7.4) solution at 37 °C on a temperature-controlled orbital shaker constantly agitated at 200 rpm. At various time (2 days, 1, 2 and 4 weeks) points, three samples were removed, lyophilized and weighed (final mass). The mass loss was calculated from the initial and final mass values.

### 2.9. Mechanical Analysis

Mechanical properties of PBAE gels in equilibrium with PBS solution were determined through uniaxial compression measurements on a Zwick Roell test machine using a 500 N load cell in a thermostated room at 23 ± 2 °C. The cylindrical gel samples were cut into cubic samples with dimensions 3x4x4 mm. Before the tests, a complete contact between the gel specimen and the metal plate was provided by applying an initial compressive force of 0.01 N. The tests were carried out at a constant cross-head speed of 1 mm·min$^{-1}$. Compressive stress is presented by

its nominal value $\sigma_{nom}$, which is the force per cross-sectional area of the undeformed gel specimen, while strain is given by $\varepsilon$ which is the change in the specimen length with respect to its initial length. Young's modulus $E$ of the hydrogels was calculated from the slope of stress−strain curves between 10 and 15% compressions. For reproducibility, at least three samples were measured for each gel and the results were averaged.

### 2.10. *In vitro* cytotoxicity assay

NIH 3T3 cells were used to evaluate the cytotoxicity of the degradation products of the prepared gels. The cells were cultured in RPMI 1640 complete medium supplemented with 10% (v/v) FBS and 1% (v/v) pen-strep in 5% $CO_2$-humidified incubator at 37 ºC and passaged every 2-3 days. For the cytotoxicity assay, the cells were seeded at a density of $10^4$ cells/well in RPMI 1640 complete medium into 96-well plates and incubated at 37 ºC in 5% $CO_2$ atmosphere until 60-80% confluency. Then, the degradation products of the hydrogels in different concentrations ranging between 10-200 µg/mL were introduced into the wells. After 24 h further incubation, the cell viability was assessed using MTT colorimetric assay by the addition of 50 µL of MTT solution (5 mg/mL in PBS) into each well with 150 µL of culture medium and incubated for 4 more hours. The purple formazan crystals formed as a result of mitochondrial activity in viable cells were dissolved with ethanol:DMSO (1:1 v/v) mixture. Each sample's absorbance at 600 nm with a reference reading at 630 nm was recorded using a BioTek ELX800 microplate reader (BioTek Instruments Inc., Winooski, VT, USA). Cells which were not exposed to degradation products of gels were used as controls. 100% viability was assumed for the control cells; hence the relative cell viability was calculated from equation (2):

$$Cell\ viability\ (\%) = \frac{Absorbance_{sample}}{Absorbance_{control}} \text{x } 100 \qquad (n = 4) \qquad (2)$$

### 2.11. Statistical Analysis

Statistical analysis of the degradation products was conducted by using nonparametric Kruskall–Wallis one-way analysis of variance followed by multiple Dunn's comparison test of GraphPad Prism 6 software package (GraphPad Software, Inc., USA). All measurements were expressed as mean values ± standard deviation (SD). $p < 0.05$ was accepted as statistically significant difference ($n=5$).

## 3. Results and Discussion

### 3.1. Synthesis of phosphonate-functionalized diamine and PBAE macromers

A novel phosphonate-functionalized secondary diamine (PA) was synthesized via solvent-free aza-Michael reaction between 4,9-dioxa-1,12-dodecane diamine and diethyl vinylphosphonate (Fig. 1). The molar ratio of the diamine to diethyl vinylphosphonate was fixed at 1:2.1 to fully end-modify the amine and reaction was conducted at room temperature for two days (method 1). The product was obtained as a colorless viscous liquid in high yields (85 %). However, shortening the reaction to 45 minutes at 85 ºC using water as solvent also produced good results (method 2), similar to refs. 49-51. It was reported that water activates the aza-Michael addition between amines and diethyl vinylphosphonates by both hydrogen bonding between water and phosphonate group and water and the amine [52]. PA is highly soluble in polar (water, ethanol) and weakly polar solvents (chloroform, diethyl ether), but insoluble in non-polar organic solvents (hexane) (Table 1).

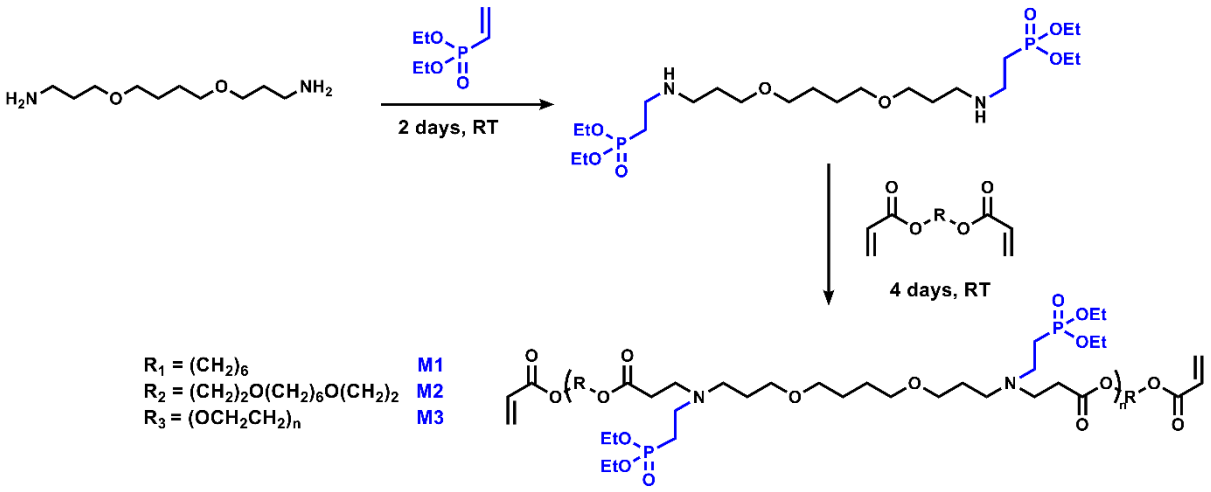


Fig. 1. Synthesis of PA and PBAE macromers M1, M2, and, M3 derived from HDDA, HDEDA, and PEGDA, respectively.

**Table 1.** Solubilities of PA and the synthesized macromers.

| Amine/Macromer | $CHCl_3$ | $H_2O$ | Petroleum ether | Diethyl Ether | Hexane | Ethanol |
|---|---|---|---|---|---|---|
| PA | + | + | + | + | - | + |
| M1 | + | - | - | - | - | + |
| M2 | + | +/- | - | - | - | + |
| M3 | + | + | - | - | - | + |

The structure of PA was confirmed by $^{1}$H-, $^{13}$C- and $^{31}$P-NMR and FTIR spectroscopy. For example, $^{1}$H NMR spectrum of the amine shows the characteristic peaks of methyl protons at 1.31 ppm, methylene protons adjacent to phosphorus at 1.94 ppm and methylene protons adjacent to nitrogen at 2.68 and 2.88 ppm (Fig. 2). The small shoulders of peaks at 1.94 and 2.88 ppm are probably due to the small amount of diadduct (6 %) formation resulting from a slight excess of diethyl vinylphosphonate (2.1 mole) used compared to 4,9-dioxa-1,12-dodecane diamine (1 mole). This side product, which is a tertiary amine, was not isolated since it will not undergo reaction with diacrylates used for PBAE synthesis. The $^{13}$C NMR spectrum of PA showed a doublet at 25.68, 27.07 ppm due to the carbon attached to phosphorus. The FTIR spectra of PA showed absorption peaks of NH, P=O and P-O at 3503, 1236, 1022 and 954 $cm^{-1}$.

Three PBAE macromers with different backbone structures were synthesized (Method 1 in experimental section; later method 2 [53] was applied to shorten the reaction time, but results from here on refer to macromers produced using method 1) from the step-growth polymerization of three diacrylates (HDDA, HDEDA and PEGDA) and PA to evaluate how chemical alterations affect final properties of the resultant networks (Fig. 1). The diacrylate:PA molar ratios were used as 1.1:1, 1.2:1 and 1.3:1 in order the obtain macromers with different molecular weights (Table 2). In the following, the macromers derived from HDDA, HDEDA and PEGDA are abbreviated as M1, M2, and M3, respectively. The hydrophilicity of the macromers increases in the order of M1 < M2 < M3. Their water-solubilities are highly dependent on the diacrylate they were synthesized from, e.g., M3 is soluble, M1 is not soluble, and M2 is slightly soluble, as expected from the order of their hydrophilicities (Table 1).

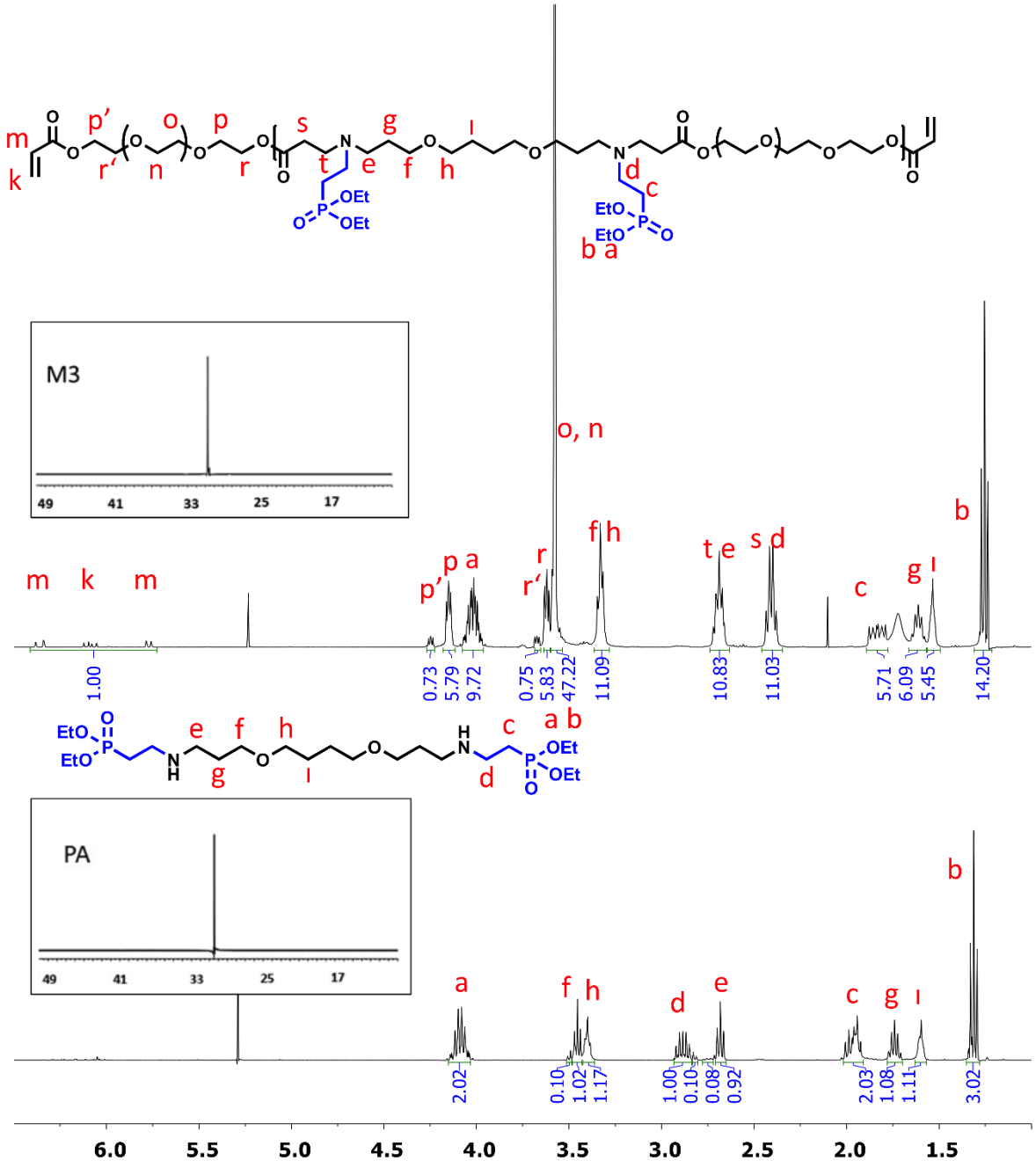


Fig. 2. $^{1}$H NMR spectra of PA and M3 (PEGDA:PA mol ratio of 1.1:1).

The structures of PBAE macromers were confirmed using $^{1}$H NMR spectroscopy (Fig. 2). The peaks at 5.8-6.5 demonstrate the maintenance of the acrylate terminal groups, and the average number of repeat units (n) of the macromers was calculated via comparison of the areas of the acrylate protons (labeled as k and m at 5.8-6.5 ppm) to phosphonate ester (labeled as b at 1.3 ppm or f, h at 3.4 ppm) protons, and was found as 5.0 ($M_n$ ~ 6300), 8.5 ($M_n$ ~ 7000) and 4.6

($M_n$ ~ 4400) for M3, M1 and M2 macromers respectively, prepared at 1.2:1 diacrylate:PA ratio. These molecular weights were higher than those obtained for their bisphosphonated analogues because of lower steric hindrance of the PA [47]. FTIR spectra of the macromers show peaks at around 1020 and 950 $cm^{-1}$ corresponding to the P-O stretching vibrations of phosphonate groups (Fig. 3).

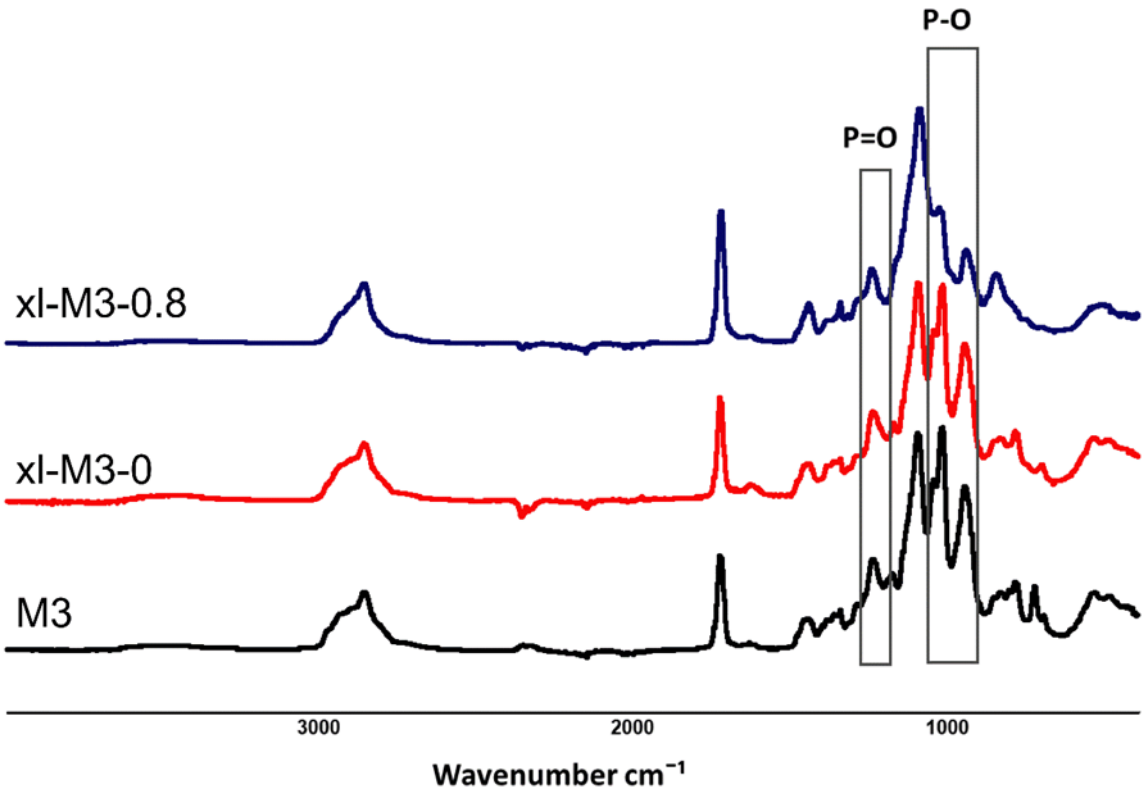


Fig. 3. FTIR spectra of M3, xl-M3-0 and xl-M3-0.8.

The solubility of PBAEs depends on solution pH due to tertiary amines in their structures. The abundance of these amine groups also give PBAEs high buffer capacity. Therefore, PBAEs can be used as pH-responsive biodegradable polymers with tunable pH transition point for drug and gene delivery carriers. Their pH sensitivity can be modified by changing the diacrylates and the amines [54,55]. In order to investigate the effect of PBAEs' structure on their pH sensitivities acid-base titration method was used (Fig. 4). All the studied polymers exhibited pH buffering capacities with slightly different buffering regions. The $pK_b$ values of M1, M2

and M3 macromers with the lowest, medium, and highest hydrophilicity, respectively, were found to be 5.5, 5.7 and 6.1, indicating effect of hydrophilicity on the $pK_b$ values. The electron donating alkyl groups lead to high electron density on the nitrogen atom and hence decrease $pK_b$, however oxygen atoms on HDEDA and PEGDA-based macromers are electron withdrawing, hence partially cancel the effect of alkyl groups. Similar behavior was observed by Song et al. [55].

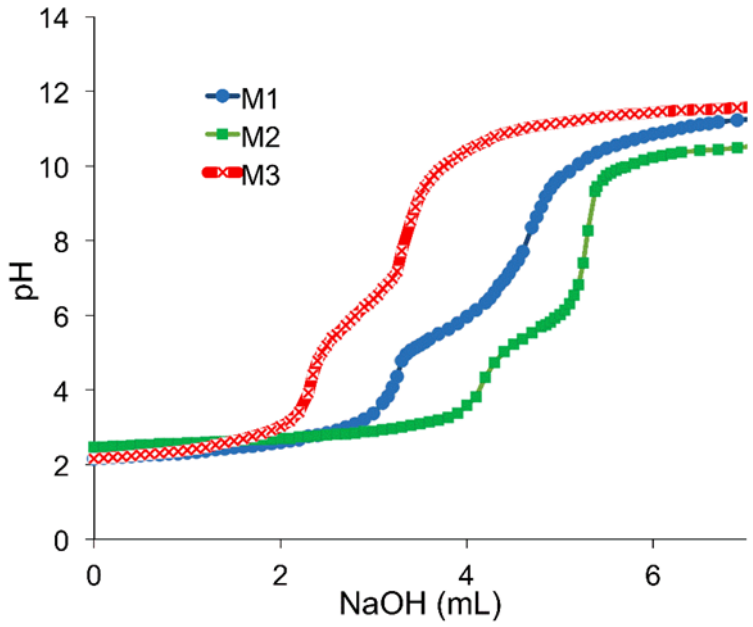


Fig. 4. Titration curves of M1, M2 and M3 macromers derived from HDDA and PEGDA, respectively.

PBAEs have low (sub-ambient) $T_g$ due to their highly flexible structures resulting from the long ethylene glycol or alkyl chains in their backbones and lack of rigid side groups [33]. The $T_g$'s of macromers were found to be -56, -59 and -60 ºC for M3, M2 and M1 macromers (Table 2).

**Table 2.** PA:diacrylate ratios, number of repeat units (n), number average molecular weights ($M_n$) and $T_g$ of the macromers.

| **Macromer** | **PA:diacrylate ratio** | **n** [a] | **$M_n$** [a] | **$T_g$ (°C)** |
|---|---|---|---|---|

| | | | | |
|---|---|---|---|---|
| M1 | 1:1.1 | 9.2 | 7500 | - |
| M1 | 1:1.2 | 8.5 | 6960 | -60 |
| M2 | 1:1.2 | 4.6 | 4360 | -59 |
| M3 | 1:1.1 | 7.1 | 8700 | - |
| M3 | 1:1.2 | 5.0 | 6280 | -56 |
| M3 | 1:1.3 | 4.1 | 5250 | - |

[a)]calculated from $^{1}$H NMR spectra

### 3.2. Synthesis of PBAE networks

The mechanical properties of biodegradable polymers usually deteriorate in parallel with the biodegradation after the polymer is implanted in the body; hence their use in load-bearing applications is problematic. To address this problem, novel biodegradable polymer designs are investigated where the degradation rate can be tuned by minor modifications of structure. For example, Safranski et al. investigated thermo-mechanical properties of semi-degradable poly(β-amino ester)-*co*-methyl methacrylate networks under simulated physiological conditions [33]. These networks showed improved mechanical properties during degradation.

The PBAE macromers synthesized in this work can be used to prepare gels with different hydrophilicities and hence, different degradation and loss profiles affecting their mechanical properties. These macromers can also control the hydrophilic/hydrophobic properties of gels they are incorporated into. To investigate these features, copolymers of the synthesized PBAE macromers with PEGDA were prepared by free radical polymerization under UV light using DMPA as photoinitiator. For comparison, the reactions were also conducted in the absence of the PEGDA cross-linker. In the following, the gel compositions were designated as xl-Mi-w, where Mi denotes type of the macromer (i = 1, 2, or 3 for HDDA, HDEDA, and PEGDA, respectively), w is the weight fraction of PEGDA in the comonomer feed (Table 3). For instance, xl-M1-0.80 presents the gel formed from HDDA macromer in the presence of 80 w% PEGDA, while xl-M1-0 denotes the gel obtained by homopolymerization of HDDA macromer (M1). After removal of unreacted macromers in ethanol, the gel fractions $W_g$ were obtained as

53-98%. FTIR analysis of the gel networks confirmed the presence of P=O and P-O peaks at 1244, 1024 and 952 $cm^{-1}$ (Fig. 3). Glass transition temperatures $T_g$ of PBAE networks with w ≤ 0.50 were around -50 °C, similar to those of the macromers they were synthesized from (Table 3). The networks with a higher PEGDA content, i.e., at w = 0.80 showed increased $T_g$ (ca. -20 °C) due to higher crosslink density resulting from the lower molecular weight of PEGDA ($M_n$ = 570 Da). However, the networks with 50% PEGDA showed two $T_g$ values (-28 and -52 °C for xl-M1-0.50; -50 and -40 °C for xl-M3-0.50) (Table 3). This behavior is interpreted as due to block copolymer structure and the two $T_g$ values correspond to the respective ones of PBAE and PEGDA, showing the heterogeneity of the components.

**Table 3.** Gel compositions, gel fraction $W_g$, degree of swelling Q, and $T_g$ values

| **Network** | **$W_g$ (%)** | ***Q* (%)** | **$T_g$ (°C)** |
|---|---|---|---|
| xl-M1-0 | 64.5±2.6 | - | -53 |
| xl-M1-0 * | 53±4.2 | - | - |
| xl-M1-0.50 | 93.2±0.1 | 38.8±3.3 | -52, -28 |
| xl-M1-0.80 | 91±2.2 | 31.3±4.0 | -21 |
| xl-M2-0 | 65.9±3.1 | - | - |
| xl-M2-0 * | 79.8±2.4 | - | - |
| xl-M2-0.50 | 66.8±2.5 | 34.5±2.0 | - |
| xl-M2-0.80 | 86.2±1.1 | 28.6±2.1 | -24 |
| xl-M3-0 | 81.3±4.8 | - | -51 |
| xl-M3-0 * | 95.6±1.3 | - | - |
| xl-M3-0.50 | 91.0±1.0 | 51.6±3.0 | -50, -40 |
| xl-M3-0.80 | 97.8±0.3 | 31.4±0.6 | -20 |

*In the synthesis of macromers, diacrylate:amine molar ratio was used as 1.1:1.

### 3.3. Swelling of networks

The gel networks were swollen in PBS (pH 7.4) to observe the influence of macromer molecular weight, amount and hydrophilicity of the macromer on their swelling behavior before and after degradation (Fig. 5). Before degradation, swelling degrees were low (28.6-51.6%) because both

the macromer and PEGDA components of the networks are crosslinkers. Moreover, the amount of the macromer does not influence the swelling percentages except xl-M3-0.50. The presence of HDEDA vs. HDDA in the backbone of the PBAE macromer was found to not make an important difference in swelling; indicating that the hydrophilicities of the phosphonate-functionalities and PEGDA determine the swelling. However, when PEGDA-based PBAE macromer is used, the increased amount of PEGDA does make a difference, leading to the exception of xl-M3-0.50. This assertion is confirmed by the data of networks with 20 w% PBAE macromers ($w$ = 0.80), where the swelling percentages were found to be similar to those of the 50% ($w$ = 0.5) samples, the M3 sample showing only slightly higher swelling, since it aquires slightly higher amount of PEGDA with respect to M1 and M2 samples.

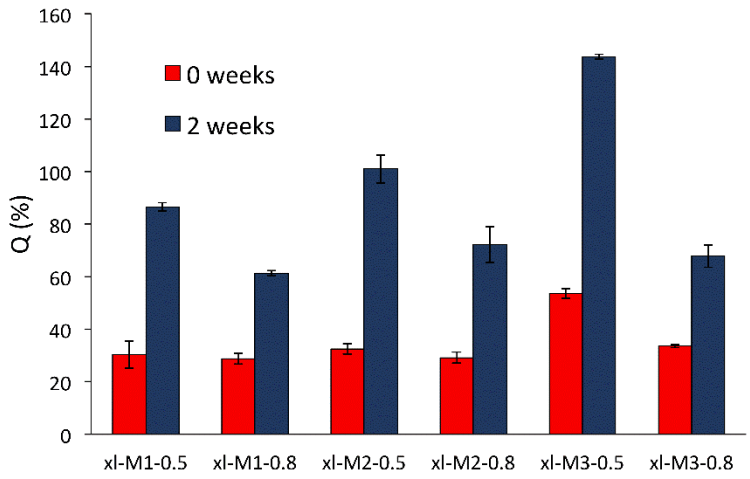


Fig. 5. Swelling percentages (Q) of the gels before and after degradation for 2 weeks.

The degradation of the gels over time have been monitored by the time-dependent swelling measurements. After degradation in PBS for 2 weeks, the swelling degree of degraded gels increased compared to those of non-degraded ones with the same composition (Fig. 5). While xl-M3-0.50 gel swelled 51.6% initially, after 2 weeks of degradation its swelling percentage was found to be about 143.7%. The swelling of the degraded gels increases with an increase in both PBAE content and its hydrophilicity, which also determines degradation rate of the gels.

An explanation is that degradation destroys the integrity of the hydrogel and enhances the penetration of water into the gel. This explanation was checked using mechanical tests conducted on virgin and degraded gels, as will be discussed later.

### 3.4. Degradation of networks

Tissue-engineering scaffolds should both guide the proliferating cells to form new tissue, and disappear when their job is completed. Therefore, the degradation rate of the scaffold should be tuned such that it turns slowly into a porous matrix into which molecules can diffuse, cells enter, adhere, proliferate and interconnect; and breaks apart at the appropriate time. Hence it is important to investigate degradation behavior of any new candidates for tissue-scaffold materials.

Fig. 6 shows degradation of the PBAE gels in PBS (pH 7.4) at 37 °C. The dependence of degradation rate on PBAE structure is clearly evident. The gels formed from more hydrophobic PBAE macromer degrade slower; degradation rates were found to increase in the following order: xl-M1 < xl-M2 < xl-M3, in accord with the order of the increase of hydrophilicity. For example, xl-M3 and xl-M1 gels degraded 80% and 15%, respectively, within 2 days. The degradation of xl-M2 gels was completed in 6 days, and xl-M3 gels in 3 days. The more hydrophobic xl-M1 network has lower water uptake and undergoes slower cleavage of ester linkages compared to the other gels. Therefore, this trend was also consistent with the swelling behavior (after 2 weeks), which is an indirect method for measurement of degradation. It was also observed that the gels formed using low molecular weight PBAE macromers of the corresponding chemical structure have significantly lower degradation rate, e.g., the lower molecular weight xl-M3 gel prepared at a PA:diacrylate ratio of 1:1.2 had less degradation (80.4%) than the higher molecular weight one, 96.7%, formed at a ratio of 1:1.1. This behavior is due to more hydrolyzable linkages in the macromer and low crosslinking density.

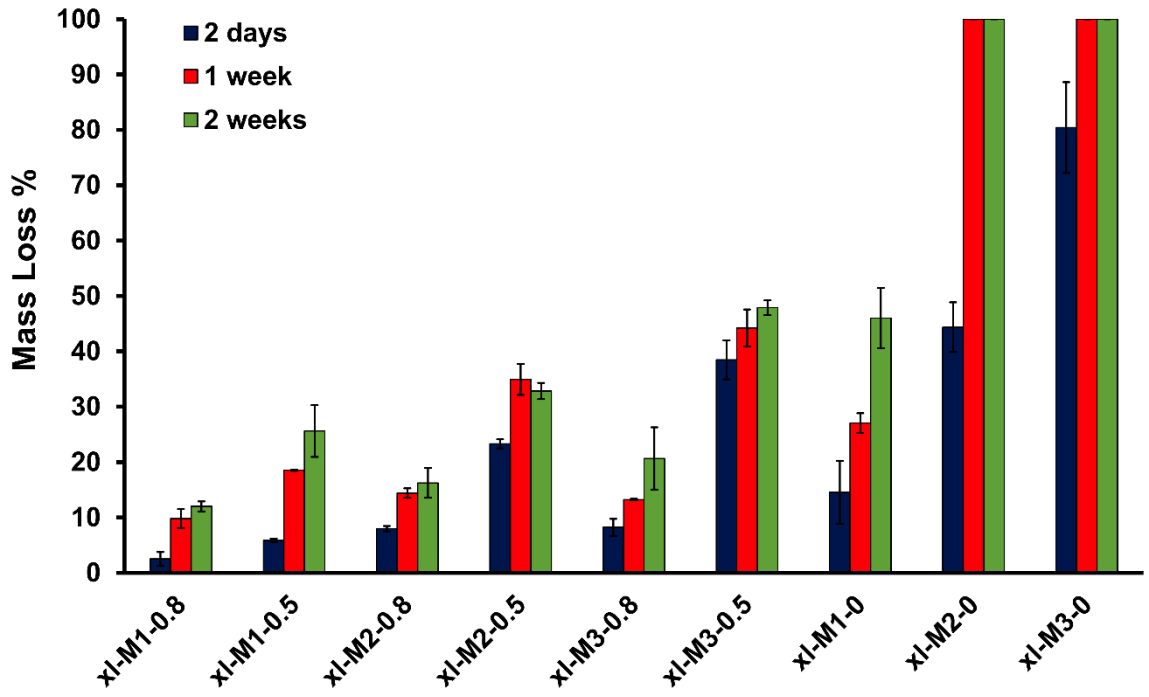


Fig. 6. The mass loss of PBAE gels and PEGDA-PBAE copolymers in 2 days, 1 week and 2 weeks in PBS.

In order to tune degradation properties of PEGDA gels, as discussed in the introduction section, PBAE macromers were copolymerized with PEGDA at different ratios. By changing the structure (hydrophilic/hydrophobic properties and molecular weight) of the macromers, gels with mass losses ranging from 12.0 % to 47.9 % in 2 weeks were obtained (Fig. 6). The mass losses of gels obtained from M1 macromer with the highest hydrophobicity showed significant acceleration after 2 days. We conjecture that the water uptake for these was initially slow due to their hydrophobicity, but became faster with increased diffusion of water due to formation of the first pores, which in turn accelerated the degradation. However, the hydrophilic character of oxygen containing macromers M2 and M3 enhances their water uptake resulting in fast degradation from the beginning. For example, the mass loss of xl-M1-08 reached 26% starting from 2.5% and xl-M3-0.8 reached 32% starting from 8%; in 4 weeks.

The surface morphologies of the networks were examined at various degradation percentages by SEM (Fig. 7). The SEM images showed a smooth surface before degradation, which became porous and rough after degradation. The xl-M3-0 network prepared without PEGDA comonomer after 80% degradation showed a sponge-like appearance with interconnected pores. However, the copolymer network xl-M3-0.80 with 15% degradation showed smaller pore size. These observations demonstrate that porosity of the networks upon degradation can be controlled by changing the PBAE content and structure.

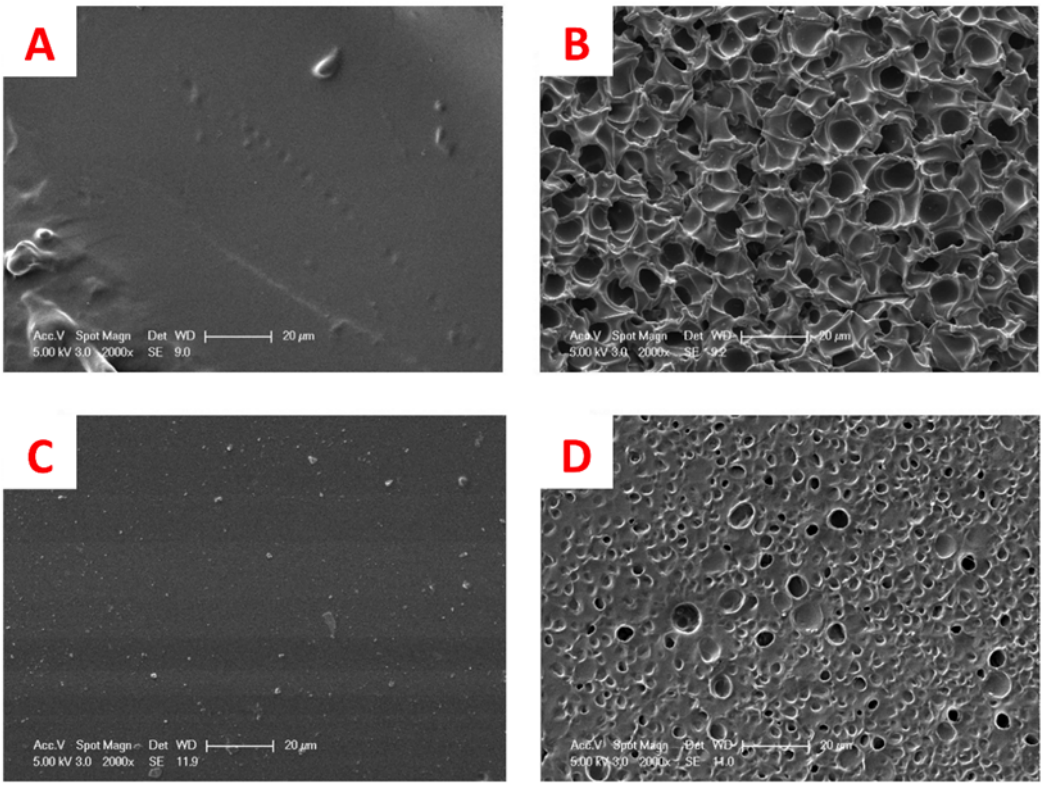


Fig. 7. SEM images of networks: xl-M3-0 before (A) and after 80% degradation (B); xl-M3-0.80 before (C) and after 15% degradation (D).

In order to determine degradation mechanism of the networks, NMR and FTIR spectra of the degradation products of two of the PBAE networks, xl-M3-0 and xl-M2-0, were investigated after full degradation in water. FTIR spectrum of the degradation products of xl-M3-0 showed i) formation of a peak at 3481 $cm^{-1}$ (due to OH groups), ii) broadening and decreasing intensity of C=O peak and formation of a new broad peak at 1594 $cm^{-1}$ (due to formation of COOH

groups) (Fig. S1). $^{1}$H NMR spectrum of the same sample indicated that the integral of the peak at 4.25 ppm due to the methylene protons adjacent to the ester ($COOCH_2$) is decreasing and a new peak at 3.6 ppm, due to the methylene adjacent to hydroxyl group ($HOCH_2$) is increasing. According to these results, we can say that networks degrade via hydrolysis of the multiple ester groups on the backbone into small molecule diols, bis(β-amino acids) and poly(acrylic acid) kinetic chains as reported in the literature [22,25,56].

### 3.5. Mechanical properties of PBAE gels

Mechanical properties of the gels in their equilibrium swollen states were investigated by uniaxial compression tests. Fig. 8a shows stress-strain curves of the gels prepared at PEGDA weight fractions $w$ of 0.80 (solid curves) and 0.50 (dashed curves). At $w = 0.80$, the gels sustain 25±2% compressions under around 6 MPa stresses, with a maximum fracture stress of 7.4±0.8 MPa observed for xl-M2 gel. Decreasing the weight fraction $w$ from 0.80 to 0.50 slightly increases the fracture strain while fracture stress decreases to 4±1 MPa indicating that incorporation of a larger amount of macromer into the gel network deteriorates their ultimate mechanical properties. Fig. 8b presenting Young's moduli $E$ of the gels reveals that, at $w$ = 0.80, $E$ is independent of the type of the macromer and remains at 27 MPa. The moduli of the hydrogels 2- to 3-fold decrease upon increasing the amount of macromer and the largest decrease was observed in xl-M2 gels.

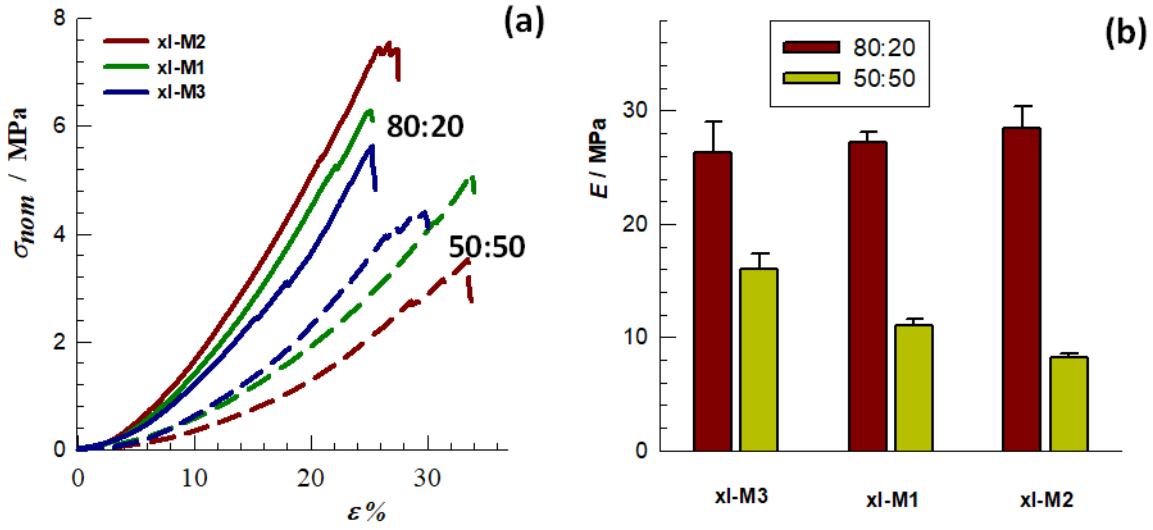


Fig. 8. (a) Stress-strain curves of the gels at w = 0.80 (solid curves) and 0.50 (dashed curves). (b) Young's moduli E of the gels formed at w = 0.80 (dark red) and 0.50 (dark yellow).

Mechanical tests were also conducted on the gel specimens subjected to various degradation times up to 4 weeks. Typical stress-strain curves of virgin and 2 weeks-degraded xl-M3 and xl-M1 gels at w = 0.50 are shown in Fig. 9a while Fig. 9b compares their moduli at various degradation times. The tests revealed that the strain at break remains almost unchanged during the course of degradation up to 2 weeks while both the fracture stress and the modulus decrease. This decrease was significant at w = 0.50 indicating that increasing amount of macromer also increases the degradation rate of the gels. Moreover, the more hydrophobic xl-M1 gel degraded slightly slower than the less hydrophobic xl-M3 gel which is in accord with the previous results.

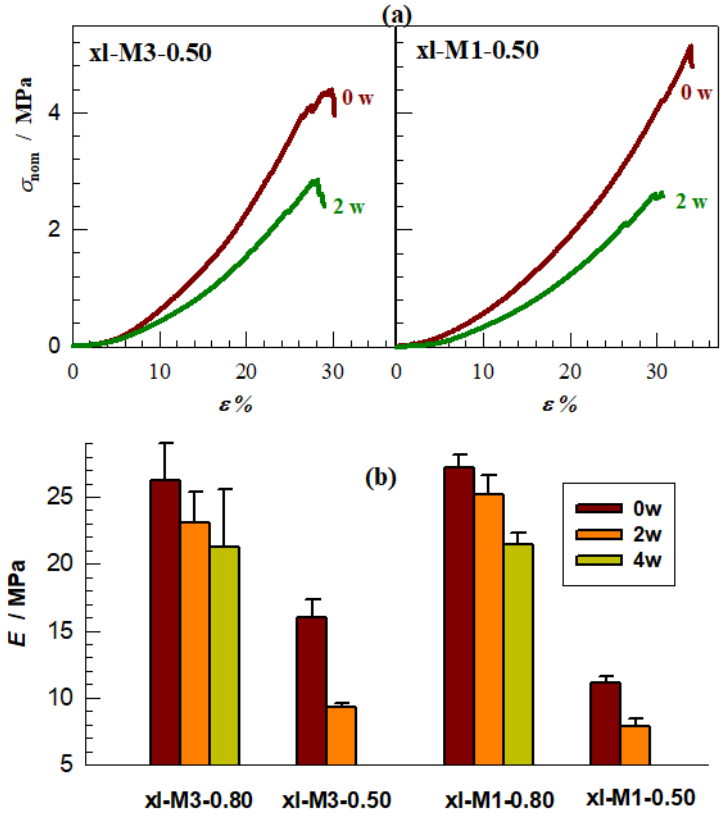


Fig. 9. (a) Typical stress-strain curves of virgin and 2 weeks-degraded xl-M3 and xl-M1 gels formed from PEGDA and HDDA, respectively. w = 0.50. (b) The modulus E of gels at various degradation times.

Because both the degree of swelling $Q$ of the hydrogels and their moduli $E$ change during degradation, a direct evidence of the change in the network structure can be obtained from their effective cross-link densities $\nu_e$. According to the theory of rubber elasticity, Young's modulus $E$ of an affine network is related to its cross-link density $\nu_e$ by [57,58]

$$E = 3\nu_e RT\left(\nu_2\right)^{1/3}\left(\nu_2^0\right)^{2/3} \tag{3}$$

where $\nu_2^0$ and $\nu_2$ are the volume fractions of cross-linked polymer just after the gel preparation and at the state of the measurements, respectively, $R$ and $T$ are in their usual meanings. Although the gels were prepared under solvent-free condition, the presence of unreacted macromers after gelation acting as a diluent leads to a decrease of $\nu_2^0$ below unity. For the following calculations,

we estimated $\nu_2^0$ as equal to the gel fraction $W_g$. Moreover, $\nu_2$ was calculated from the degree of swelling $Q$ as:

$$\nu_2 = \left(1 + Q\, d_2 / d_1\right)^{-1} \qquad (4)$$

where $d_1$ is the density of water (1 g $mL^{-1}$) and $d_2$ is the polymer density measured as 0.82 g $mL^{-1}$. By substituting $Q$ and $E$ values into eqs 3 and 4, we estimated the cross-link density $\nu_e$ of the gels at various times. Fig. 10a shows the variation of $\nu_e$ of xl-M1 and xl-M3 gels with the degradation time. The fraction of degraded network chains calculated as 1- $\nu_e / \nu_{e,o}$, where $\nu_{e,o}$ is the initial cross-link density at time = 0, is shown in Fig. 10b. During the first two weeks, the crosslink density of the gels with $w$ = 0.80 does not change much (filled symbols), and even remains unchanged for the M1 gel with the highest hydrophobicity. In contrast, $\nu_e$ of the gels with $w$ = 0.50 rapidly decreases while the fraction of degraded network chain increases. After 2 weeks, around 20 and 30% of the network chains contributing to the gel elasticity are lost in xl-M1 and xl-M3 gels, respectively. These results show the significant effect of both the type and the amount of the macromers on the degradability of the gels.

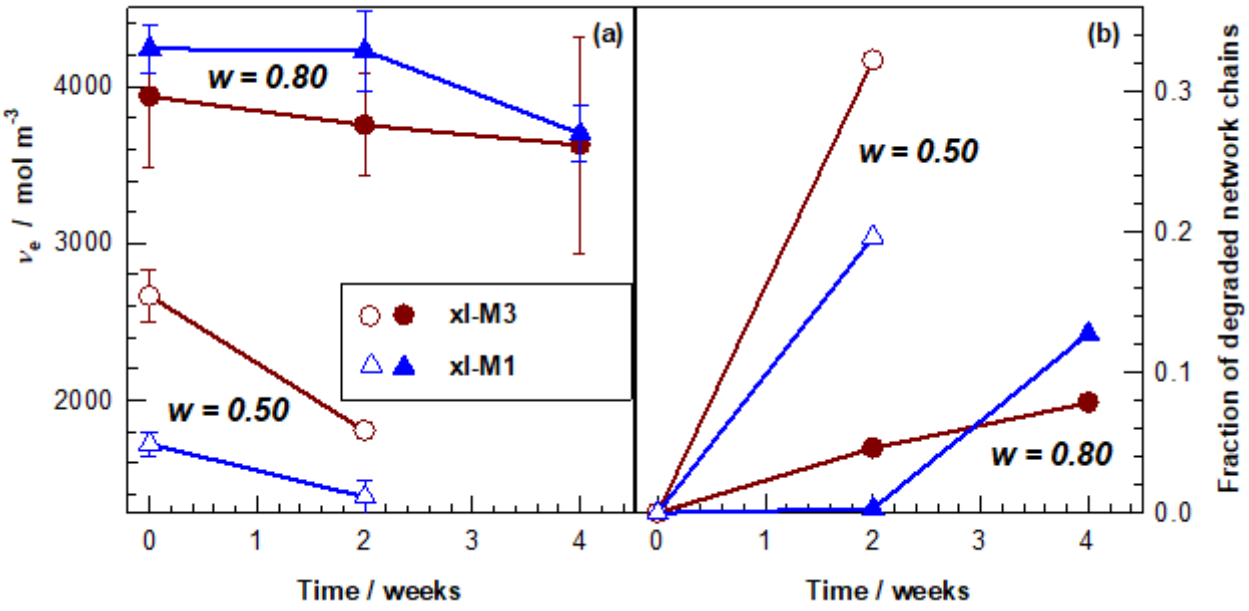

Fig. 10. The cross-link density $\nu_e$ of the hydrogels (a) and the fraction of degraded network chains, 1- $\nu_e / \nu_{e,o}$, (b) both plotted against the degradation time. Empty symbols: w = 0.5, filled symbols: w = 0.8.

### 3.6. *In vitro* cytotoxicity of polymer degradation products

The cytotoxicity measurement is an important step to determine the biocompatibility of a material for biomedical applications. The cytotoxicity of the degradation products of PBAE gels was investigated on NIH 3T3 cells using MTT cell metabolic activity assay (Fig. 11). Following ISO standard 10993–5 [59], the cells in RPMI-1640 culturing medium was used to evaluate if there is a cytotoxic response to degradation products. Cells cultured under normal conditions without any material were used as a control. There was no significant difference between toxicities (cell viability > 80%) of PBAE degradation products at any concentrations against NIH 3T3. These values were also found not to be significantly different than those of control, indicating the synthesized PBAE gels as non-toxic materials.

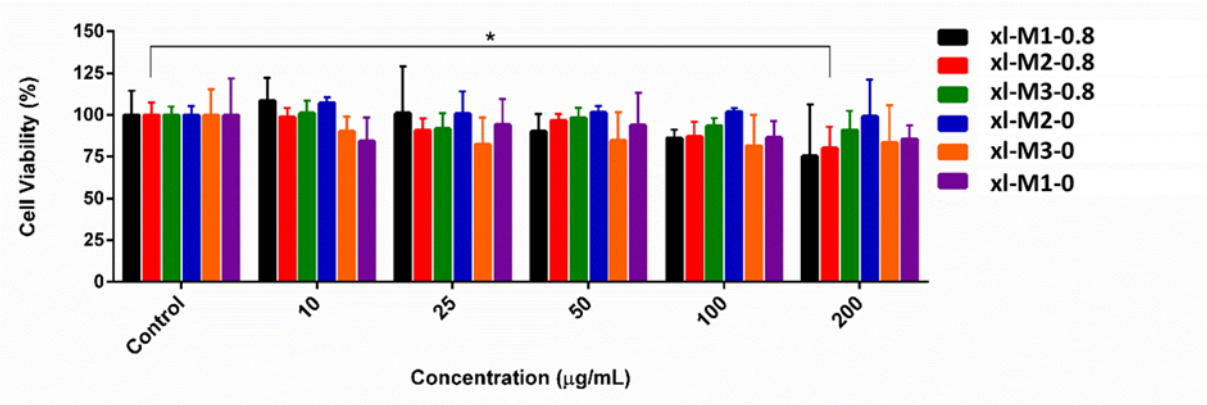


Fig. 11. The effect of degradation products on cell viability of NIH 3T3 mouse embryonic fibroblast cells. Cells were treated with different concentrations of the products for 24 h. The cell viability test was performed by MTT assay (±SD; n = 5; $p < 0.05$ compared with all concentrations).

## 4. Conclusions

We demonstrated that novel phosphonate-functionalized secondary diamines with different spacers can be easily synthesized by Michael addition reaction and can be used for the synthesis

of novel phosphonate-functionalized PBAEs. It was observed that by changing the PBAE structure it is possible to obtain homo- and copolymeric gels of different swelling, degradation and mechanical properties. Swelling percentages of PEGDA gels before degradation were independent of the PBAE crosslinker identity but after degradation increased with an increase in PBAE crosslinker content and was dependent on the type of crosslinker. The degradation rates of PBAE gels were controlled by the hydrophilicity (M1 < M2 < M3) and molecular weight of the PBAE macromer. Their degradabilities are about two to ten times higher than that of PEGDA gels containing 20 and 50 w % of PBAEs in two days. Mechanical tests reveal that PBAE gels prepared at a PEGDA weight fraction of 0.80 sustain 25±2% compressions under around 6 MPa stresses. Decreasing PEGDA weight fraction slightly increases the fracture strain while fracture stress decreases to 4±1 MPa indicating that incorporation of a larger amount of macromer into the gel network deteriorates their ultimate mechanical properties. The results also show that the extent of decrease of the gel cross-link density during degradation correlates strongly and positively with increasing amount and hydrophilicity of the PBAE macromers. The cytotoxicity study of the degradation products on NIH 3T3 mouse embryonic fibroblast cells supports the biocompatibility of these materials for biomedical applications. Overall, these three PBAE macromers and their homo- and copolymers show promise to be used as scaffolds for tissue engineering applications.

**Acknowledgement**

The authors thank TUBITAK (114Z926) for financial support. O.O. thanks the Turkish Academy of Sciences (TUBA) for the partial support.

**Appendix**

FTIR spectra of PA, M3, xl-M3-0 (before degradation) and xl-M3-0 (after 2 days of degradation in water).

The raw/processed data required to reproduce these findings cannot be shared at this time due to technical or time limitations.

## References


[1] A. Hatefi, B. Amsden, Biodegradable injectable in situ forming drug delivery systems, J. Control. Release. 80 (2002) 9-28.

[2] K. T. Nguyen, J. L. West, Photopolymerizable hydrogels for tissue engineering applications, Biomaterials 23 (2002) 4307-4314.

[3] M. B. Chan-Park , A. P. Zhu, J. Y. Shen, A. L. Fan, Novel Photopolymerizable biodegradable triblock polymers for tissue engineering scaffolds: Synthesis and characterization, Macromol. Biosci. 4 (2004) 665-673.

[4] R. Censi, S. van Putten, T. Vermonden, P. di Martino, C. F. van Nostrum, M. C. Harmsen, R. A. Bank, W. E. Hennink, The tissue response to photopolymerized PEG-p(HPMAm-lactate)-based hydrogels, J. Biomed. Mater. Res. A. 97A **(**2011) 219-229.

[5] R. A. Hakala, H. Korhonen, V. V. Meretoja, J. V. Seppälä, Photo-cross-linked biodegradable poly(ester anhydride) networks prepared from alkenylsuccinic anhydride functionalized poly(ε-caprolactone) precursors, Biomacromolecules 12 (2011) 2806-2814.

[6] S. Kasetaite, J. Ostrauskaite, V. Grazuleviciene, D. Bridziuviene, R. Budreckiene, E. Rainosalo, Biodegradable photocross-linked polymers of glycerol diglycidyl ether and structurally different alcohols, React. Funct. Polym. 122 (2018) 42-50.

[7] R. Loth, T. Loth, K. Schwabe, R. Bernhardt, M. Schulz-Siegmund, M. C. Hacker, Highly adjustable biomaterial networks from three-armed biodegradable macromers, Acta Biomater. 26 (2015) 82-96.

[8] D. M. Lynn, R. Langer, Degradable poly(β-amino esters): Synthesis, characterization, and self-assembly with plasmid DNA, J. Am. Chem. Soc. 122 (2000) 10761-10768.

[9] D. M. Lynn, D. G. Anderson, D. Putnam, R. Langer, Accelerated discovery of synthetic transfection vectors: Parallel synthesis and screening of a degradable polymer library, J. Am. Chem. Soc. 123 (2001) 8155-8156.

[10] D. G. Anderson, D. M. Lynn, R. Langer, Semi-automated synthesis and screening of a large library of degradable cationic polymers for gene delivery, Angew. Chem. Int. Ed. 42 (2003) 3153-3158.

[11] N. S. Bhise, R. S. Gray, J. C. Sunshine, S. Htet, A. J. Ewald, J. J. Green, The relationship between terminal functionalization and molecular weight of a gene delivery polymer and transfection efficacy in mammary epithelial 2-D cultures and 3-D organotypic cultures, Biomaterials 31 (2010) 8088-8096.

[12] A. A. Eltoukhy, D. J. Siegwart, C. A. Alabi, J. S. Rajan, R. Langer, D. G. Anderson, Effect of molecular weight of amine end-modified poly(β-amino ester)s on gene delivery efficiency and toxicity, Biomaterials 33 (2012) 3594-3603.

[13] J. Zhao, P. Huang, Z. Wang, Y. Tan, X. Hou, L. Zhang, C-Y. He, Z-Y. Chen, Synthesis of amphiphilic poly(β-amino ester) for efficiently minicircle DNA delivery in vivo, ACS Appl. Mater. Interfaces 8 (2016) 19284-19290.

[14] J-Y. Huang, Y. Gao, L. Cutlar, J. O'Keeffe-Ahern, T. Zhao, F-H. Lin, D. Zhou, S. McMahon, U. Greiser, W. Wang, W. Wang, Tailoring highly branched poly(β-amino ester)s: a synthetic platform for epidermal gene therapy, Chem. Commun. 51 (2015) 8473-8476.

[15] N. Segovia, P. Dosta, A. Cascante, V. Ramos, S. Borros, Oligopeptide-terminated poly(β-amino ester)s for highly efficient gene delivery and intracellular localization, Acta Biomater. 10 (2014) 2147-2158.

[16] C. T. Huynh, M. K. Nguyen, J. H. Kim, S. W. Kang, B. S. Kim, D. S. Lee, Sustained delivery of doxorubicin using biodegradable pH/temperature sensitive poly(ethylene glycol)-poly(β-amino ester urethane) multiblock copolymer hydrogels, Soft Matter 7 (2011) 4974-4982.

[17] P. D. Fisher, J. Clemens, J. Z. Hilt, D. A. Puleo, Multifunctional poly(*β*-amino ester) hydrogel microparticles in periodontal *in situ* forming drug delivery systems, Biomed. Mater. 11 (2016) 025002.

[18] S. Perni, P. Prokopovich, Poly-beta-amino-esters nano-vehicles based drug delivery system for cartilage, *Nanomedicine: NBM* 13 (2017) 539-548.

[19] S. Tang, Q. Yin, Z. Zhang, W. Gu, L. Chen, H. Yu, Y. Huang, X. Chen, M. Xu, Y. Li, Co-delivery of doxorubicin and RNA using pH-sensitive poly (β-amino ester) nanoparticles for reversal of multidrug resistance of breast cancer, Biomaterials 35 (2014) 6047-6059.

[20] Z. Duan, Y-J. Gao, Z-Y. Qiao, G. Fan, Y. Liu, D. Zhang, H. Wang, A photoacoustic approach for monitoring the drug release of pH-sensitive poly(β-amino ester)s, J. Mater. Chem. B, 2 (2014) 6271-6282.

[21] J. S. Lee, X. Deng, P. Han, J. Cheng, Dual stimuli-responsive poly(β-amino ester) nanoparticles for on-demand burst release, Macromol. Biosci. 15 (2015) 1314-1322.

[22] D. G. Anderson, C. A. Tweedie, N. Hossain, S. M. Navarro, D. M. Brey, K. J. Van Vliet, R. Langer, J. A. Burdick, A combinatorial library of photocrosslinkable and degradable materials, Adv. Mater. 18 (2006) 2614-2618.

[23] A. M. Hawkins, T. A. Milbrandt, D. A. Puleo, J. Z. Hilt, Synthesis and analysis of degradation, mechanical and toxicity properties of poly(β-amino ester) degradable hydrogels, Acta Biomater. 7 (2011) 1956-1964.

[24] D. M. Brey, I. Erickson, J. A. Burdick, Influence of macromer molecular weight and chemistry on poly(β-amino ester) network properties and initial cell interactions, J. Biomed. Mater. Res. A. 85 (2008) 731-741.

[25] D. M. Brey, J. L. Ifkovits, R. I. Mozia, J. S. Katz, J. A. Burdick, Controlling poly(β-amino ester) network properties through macromer branching, Acta Biomater. 4 (2008) 207-217.

[26] A. R. Tan, J. L. Ifkovits, B. M. Baker, D. M. Brey, R. L. Mauck, J. A. Burdick, Electrospinning of photocrosslinked and degradable fibrous scaffolds, J. Biomed. Mater. Res. A. 87 (2008) 1034-1043.

[27] R. B. Metter, J. L. Ifkovits, K. Hou, L. Vincent, B. Hsu, L. Wang, R. L. Mauck, J. A. Burdick, Biodegradable fibrous scaffolds with diverse properties by electrospinning candidates from a combinatorial macromer library, Acta Biomater. 6 (2010) 1219-1226.

[28] G. Gonzales, X. Fernandez-Francos, A. Serra, M. Sangermano, X. Ramis, Environmentally-friendly processing of thermosets by two-stage sequential aza-Michael addition and free-radical polymerization of amine–acrylate mixtures, Polym. Chem. 6 (2015) 6987-6997.

[29] A. M. Hawkins, T. A. Milbrandt, D. A. Puleo, J. Z. Hilt, Composite hydrogel scaffolds with controlled pore opening via biodegradable hydrogel porogen degradation, J. Biomed. Mater. Res. A. 102A (2014) 400-412.

[30] Y. Zhang, R. Wang, Y. Hua, R. Baumgartner, J. Cheng, Trigger-responsive poly(β-amino ester) hydrogels, ACS Macro Lett. 3 (2014) 693-697.

[31] R. A. McBath, D. A. Shipp, Swelling and degradation of hydrogels synthesized with degradable poly(β-amino ester) crosslinkers, Polym. Chem. 1 (2010) 860-865.

[32] D. L. Safranski, D. Weiss, J. B. Clark, W. R. Taylor, K. Gall, Semi-degradable poly(β-amino ester) networks with temporally-controlled enhancement of mechanical properties, Acta Biomater. 10 (2014) 3475-3483.

[33] D. L. Safranski, J. C. Crabtree, Y. R. Huq, K. Gall, Thermo-mechanical properties of semi-degradable poly(β-amino ester)-co-methyl methacrylate networks under simulated physiological conditions, Polymer 52 (2011) 4920-4927.

[34] B. R. Orellana, M. V. Thomas, T. D. Dziubla, N. M. Shah, J. Z. Hilt, D. A. Puleo, Bioerodible calcium sulfate/poly(β-amino ester) hydrogel composites, J. Mech. Behav. Biomed. Mater. 26 (2013) 43-53.

[35] S. Monge, B. Canniccioni, A. Graillot, J-J. Robin, Phosphorus-containing polymers: A great opportunity for the biomedical field, Biomacromolecules 12 (2011) 1973-1982.

[36] W. Chu, Y. Huang, C. Yang, Y. Liao, X. Zhang, M. Yan, S. Cui, C. Zhao, Calcium phosphate nanoparticles functionalized with alendronate-conjugated polyethylene glycol (PEG) for the treatment of bone metastasis, Int. J. Pharm. 516 (2017) 352-363.

[37] Z. Sarayli Bilgici, S. B. Turker, D. Avci, Novel bisphosphonated methacrylates: Synthesis, polymerizations, and interactions with hydroxyapatite, Macromol. Chem. Phys. 214 (2013) 2324-2335.

[38] A. Altin, B. Akgun, Z. Sarayli Bilgici, S. B. Turker, D. Avci, Synthesis, photopolymerization, and adhesive properties of hydrolytically stable phosphonic acid-containing (meth)acrylamides, J. Polym. Sci. A Polym. Chem. 52 (2014) 511-522.

[39] X. Cui, Y. Koujima, H. Seto, T. Murakami, Y. Hoshino, Y. Miura, Inhibition of bacterial adhesion on hydroxyapatite model teeth by surface modification with PEGMA-Phosmer copolymers, ACS Biomater. Sci. Eng. 2 (2016) 205-212.

[40] J. Tan, R. A. Gemeinhart, M. Ma, W. M. Saltzman, Improved cell adhesion and proliferation on synthetic phosphonic acid-containing hydrogels, Biomaterials 26 (2005) 3663-3671.

[41] M. Dadsetan, M. Giuliani, F. Wanivenhaus, B. M. Runge, J. E. Charlesworth, M. J. Yaszemski, Incorporation of phosphate group modulates bone cell attachment and differentiation on oligo(polyethylene glycol) fumarate hydrogel, Acta Biomater. 8 (2012) 1430-1439.

[42] R. A. Gemeinhart, C. M. Bare, R. T. Haasch, E. J. Gemeinhart, Osteoblast-like cell attachment to and calcification of novel phosphonate-containing polymeric substrates, J. Biomed. Mater. Res. A. 78A (2006) 433-440.

[43] C. R. Nuttelman, D. S. W. Benoit, M. C. Tripodi, K. S. Anseth, The effect of ethylene glycol methacrylate phosphate in PEG hydrogels on mineralization and viability of encapsulated hMSCs, Biomaterials 27 (2006) 1377-1386.

[44] R. E. Dey, X. Zhong, P. J. Youle, Q. G. Wang, I. Wimpenny, S. Downes, J. A. Hoyland, D. C. Watts, J. E. Gough, P. M. Budd, Synthesis and characterization of poly(vinylphosphonic acid-coacrylic acid) copolymers for application in bone tissue scaffolds, Macromolecules 49 (2016) 2656-2662.

[45] R. E. Dey, I. Wimpenny, J. E. Gough, D. C. Watts, P. M. Budd, Poly(vinylphosphonic acid-co-acrylic acid) hydrogels: The effect of copolymer composition on osteoblast adhesion and proliferation, J. Biomed. Mater. Res. A. 106A (2018) 255-264.

[46] E. Akyol, M. Tatliyuz, F. Demir Duman, M. N. Guven, H. Yagci Acar, D. Avci, Phosphonate-functionalized poly(β-amino ester) macromers as potential biomaterials, J. Biomed. Mater. Res. A. 106A (2018) 1390-1399.

[47] M. N. Guven, M. S. Altuncu, F. Demir Duman, T. N. Eren, H. Yagci Acar, D. Avci, Bisphosphonate-functionalized poly(β-amino ester) network polymers, J. Biomed. Mater. Res. A. 105A (2017) 1412-1421.

[48] H. B. Bingol, F. Demir Duman, H. Yagci Acar, M. B. Yagci, D. Avci, Redox-responsive phosphonate-functionalized poly(β-amino ester) gels and cryogels, Eur. Polym. J. 108 (2018) 57-68.

[49] E. V. Matveeva, P. V. Petrovskii, I. L. Odinets, Efficient synthesis of racemic β-aminophosphonates via aza-Michael reaction in water, Tetrahedron Lett. 49 (2008) 6129-6133.

[50] N. Bou Orm, Y. Dkhissi, S. Daniele, L. Djakovitch, Synthesis of 2-(arylamino)ethyl phosphonic acids via the aza-Michael addition on diethyl vinylphosphonate, Tetrahedron 69 (2013) 115-121.

[51] N. G. Khusainova, D. N. Tazetdinova, I. D. Shurygin, A. R. Garifzyanov, R. A. Cherkasov, Synthesis and acid-base properties of new β-diaminophosphoryl compounds, Russ. J. Organ. Chem. 52 (2016), 1697-1699.

[52] E. V. Matveeva, P. V. Petrovskii, I. L. Odinets, Efficient synthesis of racemic β-aminophosphonates via aza-Michael reaction in water, Tetrahedron Lett. 49 (2008), 6129-6133.

[53] C-E. Yeom, M. Jeong Kim, B. Moon Kim, 1,8-Diazabicyclo[5.4.0]undec-7-ene (DBU)-promoted efficient and versatile aza-Michael addition, Tetrahedron 63 (2007) 904–909.

[54] M. S. Kim, S. J. Hwang, J. K. Han, E. K. Choi, H. J. Park, J. S. Kim, S. D. Lee, pH-Responsive PEG-poly(β-amino ester) block copolymer micelles with a sharp transition, Macromol. Rapid Commun. 27 (2006) 447-451.

[55] W. Song, Z. Tang, M. Li, S. Lv, H. Yu, L. Ma, X. Zhuang, Y. Huang, X. Chen, Tunable pH-Sensitive poly(β-amino ester)s synthesized from primary amines and diacrylates for intracellular drug delivery, Macromol. Biosci. 12 (2012) 1375-1383.

[56] P. Gupta, C. Lacerda, V. Patil, D. Biswal, P. Wattamwar, J. Zach Hilt, T. D. Dziubla, Degradation of Poly(β-Amino Ester) Gels in Alcohols Through Transesterification: Method to Conjugate Drugs to Polymer Matrices, J. Polym. Sci. A Polym. Chem. 55 (2017) 2019–2026.

[57] L. R. G. Treloar, *The Physics of Rubber Elasticity*, University Press, Oxford, **1975**.

[58] P. J. Flory, *Principles of Polymer Chemistry*, Cornell University Press, Ithaca, NY, **1953**.

[59] R.F. Wallin, E. Arscott, A practical guide to ISO 10993–5: cyotoxicity, Med. Device Diagn. Ind. 20 (1998) 96–98.

## Figure Captions

**Fig. 1.** Synthesis of PA and PBAE macromers M1, M2, and, M3 derived from HDDA, HDEDA, and PEGDA, respectively.

**Fig. 2.** $^{1}$H NMR spectra of PA and M3 (PEGDA:PA mol ratio of 1.1:1).

**Fig. 3**. FTIR spectra of M3, xl-M3-0 and xl-M3-0.8.

**Fig. 4.** Titration curves of M1, M2 and M3 macromers derived from HDDA and PEGDA, respectively.

**Fig. 5**. Swelling percentages (Q) of the gels before and after degradation for 2 weeks.

**Fig. 6.** The mass loss of PBAE gels and PEGDA-PBAE copolymers in 2 days, 1 week and 2 weeks in PBS.

**Fig. 7.** SEM images of networks: xl-M3-0 before (A) and after 80% degradation (B); xl-M3-0.80 before (C) and after 15% degradation (D).

**Fig. 8.** (a) Stress-strain curves of the gels at w = 0.80 (solid curves) and 0.50 (dashed curves). (b) Young's moduli E of the gels formed at w = 0.80 (dark red) and 0.50 (dark yellow).

**Fig. 9.** (a) Typical stress-strain curves of virgin and 2 weeks-degraded xl-M3 and xl-M1 gels formed from PEGDA and HDDA, respectively. w = 0.50. (b) The modulus E of gels at various degradation times.

**Fig. 10.** The cross-link density $\nu_e$ of the hydrogels (a) and the fraction of degraded network chains, 1- $\nu_e / \nu_{e,o}$, (b) both plotted against the degradation time. Empty symbols: w = 0.5, filled symbols: w = 0.8.

**Fig. 11**. The effect of degradation products on cell viability of NIH 3T3 mouse embryonic fibroblast cells. Cells were treated with different concentrations of the products for 24 h. The cell viability test was performed by MTT assay (±SD; n = 5; $p < 0.05$ compared with all concentrations).

## Tables

**Table 1.** Solubilities of PA and the synthesized macromers.

**Table 2.** PA:diacrylate ratios, number of repeat units (n), number average molecular weights ($M_n$) and $T_g$ of the macromers.

**Table 3.** Gel compositions, gel fraction $W_g$, degree of swelling Q, and $T_g$ values.

## Supporting Information

**Structure-property relationships of novel phosphonate-functionalized networks and gels of poly(β-amino esters)**

Seckin Altuncu, Fatma Demir Duman, Umit Gulyuz, Havva Yagci Acar, Oguz Okay, Duygu Avci

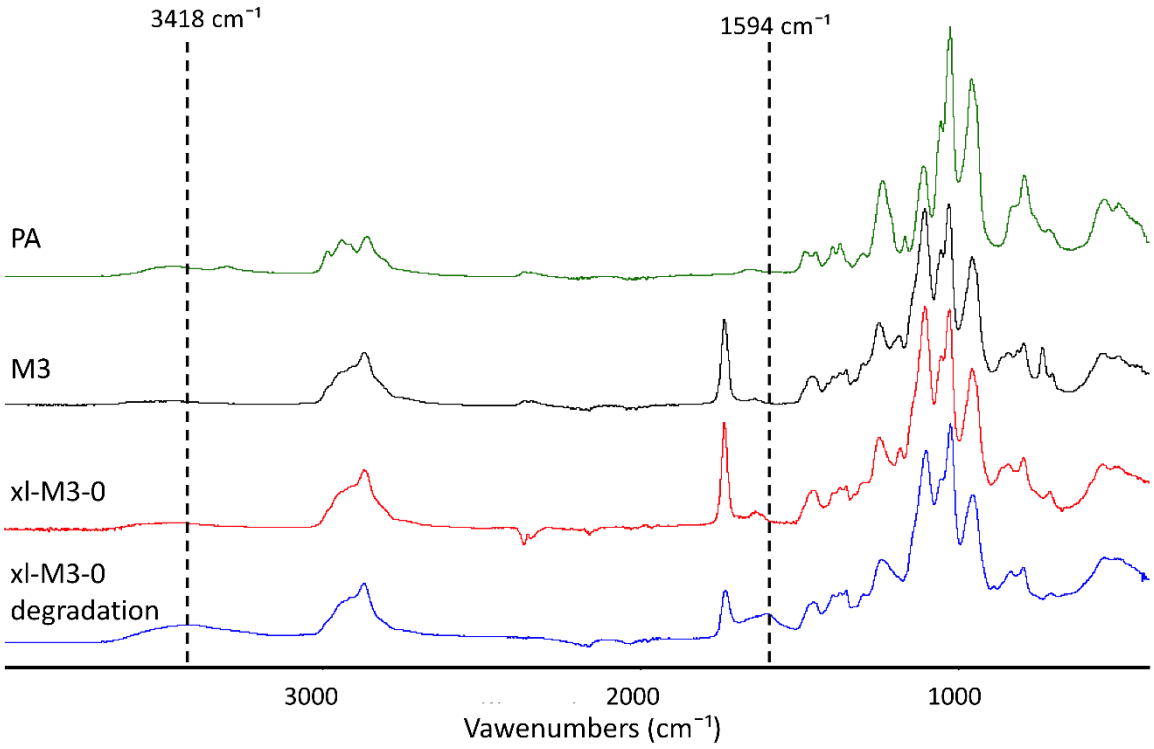


Fig. S1. FTIR spectra of PA, M3, xl-M3-0 (before degradation) and xl-M3-0 (after 2 days of degradation in water).